JGP Journal of General Physiology

COMMENTARY

Chloride Channels and Transporters

Locking the TMEM16A chloride channel into its conductive state

Zhang Feng[1]

A TM3–TM4 hydrophobic patch couples TM4 remodeling to TMEM16A channel gating and sheds light on TMEM16 family divergence.

The Ca^{2+}-activated chloride channel TMEM16A is a key mediator of epithelial Cl^- secretion, smooth muscle contraction, sensory signaling, and membrane excitability (Caputo et al., 2008; Schroeder et al., 2008; Yang et al., 2008). Because these physiological processes require tightly regulated Ca^{2+}-dependent Cl^- flux, understanding how Ca^{2+} binding is coupled to TMEM16A pore opening remains a central question. Yet, structural analyses of TMEM16A have not revealed a fully conductive state, leaving its gating mechanism an open question. Previous work identified a hydrophobic gate formed by residues on TM4 and TM6, two pore-lining helices previously reported to be involved in TMEM16A gating (Lam et al., 2021). Recent computational and functional studies, including the work by Stephens et al. in this issue of the *Journal of General Physiology* (Kostritskii et al., 2025; Stephens et al., 2026), point to local rearrangements of TM4 as a key event in pore dilation and Cl^- permeation. In particular, a π-helical transition in TM4 produces a π-bulge and a kink at L547, a key hydrophobic-gate residue near the middle of the helix that contributes to gate closure by closely contacting with I641 on TM6. This transition displaces the L547 side chain away from the pore, creating a dilated pathway for Cl^- permeation. Because such local distortions are energetically unfavorable (Kumar and Bansal, 2015), the question becomes how the novel ion-conductive TM4 conformation is stabilized. Stephens et al. identify a hydrophobic interaction network that helps stabilize the ion-conductive state of TMEM16A, highlighting the important role of TM3–TM4 interhelical interactions in TMEM16A activation.

Previous cryo-EM studies of TMEM16A have mostly captured nonconductive conformations, in which the ion permeation pathway remains closed and inaccessible from either side of the membrane. In 2022, Lam et al. reported a cryo-EM structure of TMEM16A bound to the inhibitor 1PBC (PDB: 7ZK3) (Lam et al., 2022). Interestingly, the outer part of the pore is more dilated in this structure than in previously reported structures, although the central hydrophobic gate remains closed, suggesting that it may represent a partially open conformation. In this work, Stephens et al. started MD simulations from this 1PBC-bound structure after removing the inhibitor, aiming to obtain a conductive state of TMEM16A. Upon relaxation of the inhibitor-free model in MD simulations, TMEM16A started to sample conformations in which the pore became more or less dilated. In MD trajectories that resulted in a dilated pore, TM4 underwent a π-helical transition around L547, producing a π-bulge and a kink at this position, referred to as the "upper kink" (Fig. 1 A). This conformational rearrangement has two direct consequences. First, the hydrophobic residue L547 rotates away from the pore, and the hydrophilic residue N546 rotates toward the pore axis, which leads to a reduction in the hydrophobicity of the inner pore. Second, the kink leads to an increased separation between L547 on TM4 and I641 on TM6, releasing the narrowest part of the TMEM16A pore. These observations are consistent with a recent report showing that TMEM16A opens through a π-helical transition in TM4 (Kostritskii et al., 2025), suggesting that the local TM4 rearrangement represents a characteristic feature of TMEM16A activation. Interestingly, in MD trajectories where a "lower kink" formed at E555, a glutamate located about two helical turns below L547 along TM4, the hydrophobic pore became more constricted than the starting structure. The opposite functional effects arising from conformational changes at slightly different positions within the same helix highlight the significance of local TM4 conformational rearrangements in TMEM16A activation. In this view, TM4 does not behave as a rigid helix; rather, it samples distinct bending modes and determines whether the pore becomes conductive or collapses into a nonconductive state.

In this study, the authors identified a small patch of hydrophobic interactions between the extracellular termini of TM4 and the adjacent pore-lining helix TM3 that helps stabilize the upper kink at L547 and the dilated pore. Time-lagged independent component analysis identified a hydrophobic interaction network

[1]School of Life Sciences, Nanjing Medical University, Changzhou, China.

Correspondence to Zhang Feng: feng-zhang@njmu.edu.cn.

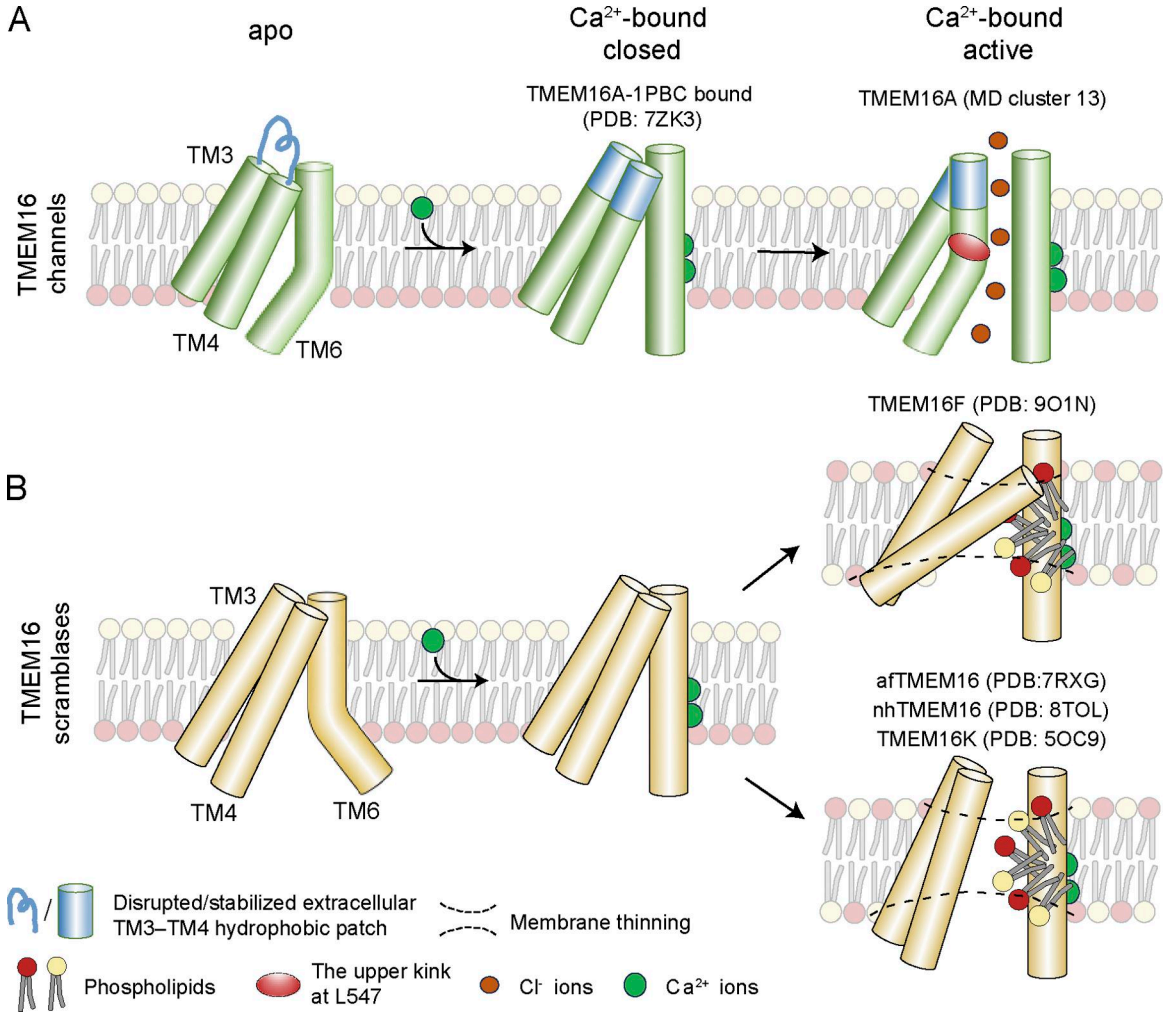

Figure 1. **Distinct TM3–TM4 interaction patterns in TMEM16 channels and scramblases. (A and B)** In the absence of Ca^{2+}, the TMEM16A channel and TMEM16 scramblases adopt similar closed conformations, with slight differences in the intracellular half of the uncoordinated TM6 (A and B). In the closed TMEM16A structure, the extracellular termini of TM3 and TM4 of TMEM16A are structured as loops (A). Ca^{2+} binding straightens TM6 in both channels and scramblases. In the inhibitor 1PBC- and Ca^{2+}-bound TMEM16A structure (PDB: 7ZK3), the extracellular TM3–TM4 termini become structured and form a hydrophobic interaction patch (A). In MD simulations initiated after removal of 1PBC, TM4 undergoes a constrained rearrangement which supports pore dilation in an ion-conductive state of TMEM16A. This arrangement involves a π-helical transition in TM4, which produces a kink at L547, referred to as the upper kink. The resulting ion-conductive state appears to be stabilized by the TM3–TM4 hydrophobic patch, consistent with the impaired channel activation caused by mutations that disrupt this network. By contrast, in the TMEM16F scramblase, the extracellular end of TM4 separates from TM3 to adopt an X-shaped conformation. In fungal TMEM16 scramblases and mammalian ER-resident scramblase TMEM16K, TM4 instead moves farther away from TM6 while maintaining interactions with TM3. These larger TM4 displacements are consistent with the ability of TMEM16 scramblases to thin the membrane to promote lipid scrambling.

that may stabilize the upper kink and promote ion permeation. To examine the role of this hydrophobic network, the authors carried out patch-clamp electrophysiology on channels mutated at two residues expected to disrupt this network. Both mutants showed markedly reduced currents and right-shifted conductance–voltage relationships, indicating impaired ion channel activation. These results suggest that the stability of the TM3–TM4 hydrophobic network is important for TMEM16A activation.

It has remained elusive how ion channels and lipid scramblases within the TMEM16 family share a similar overall architecture and Ca^{2+}-dependent activation mechanism (Feng et al., 2024; Kalienkova et al., 2021), yet perform such distinct functions. The work by Stephens et al. and others has shed light on the mechanistic basis for this functional divergence. One possibility is that TMEM16 proteins have evolved the ability to tune the stability of the TM3–TM4 interface to different extents, thereby satisfying distinct functional requirements: ion conduction in channels versus lipid scrambling in scramblases. In TMEM16A, activation appears to involve a stabilized and intact TM3–TM4 hydrophobic patch to promote pore dilation and chloride permeation. By contrast, in the activated lipid scramblase TMEM16F, the extracellular half of TM4 separates completely from TM3 and slides along TM6, resulting in an X-shaped conformation that opens a continuous pore for ion permeation and promotes local membrane thinning for lipid scrambling (Arndt et al., 2022; Feng et al., 2026). This comparison suggests

that the functional divergence between TMEM16 channels and scramblases may arise from how far TM4 rearrangement is allowed to proceed after Ca^{2+} binding: a constrained rearrangement supports pore dilation in TMEM16A (Fig. 1 A), whereas larger TM4 displacement in scramblases promotes membrane remodeling and lipid scrambling (Fig. 1 B).

Differences in the stability of TM3–TM4 interactions between channels and scramblases likely reflect the distinct physical demands of ion conduction and lipid scrambling. As a dedicated ion channel, TMEM16A appears to require a relatively limited and constrained conformational rearrangement of TM4 to dilate the pore for Cl^- permeation, while preserving a protein-lined pore compatible with Cl^- selectivity. For scramblases, however, such a local rearrangement may not be sufficient. Current models suggest that TMEM16 scramblases enable lipid scrambling by inducing membrane deformation and thinning (Falzone et al., 2022; Feng et al., 2019), thereby lowering the energy barrier for lipid headgroup translocation across the bilayer. This functional requirement could involve Ca^{2+}-induced TM4 conformational rearrangement proceeding beyond local pore dilation to drive broader remodeling of the protein-membrane interface. In activated TMEM16F, this is achieved through separation of the extracellular half of TM4 from TM3 and its sliding along TM6 while maintaining limited contact with TM6 (Fig. 1 B). By contrast, in fungal TMEM16 scramblases and the ER-resident scramblase TMEM16K, TM4 moves laterally away from TM6, resulting in a fully membrane-exposed open groove and therefore more pronounced membrane thinning (Fig. 1 B). Thus, although TMEM16 family members use Ca^{2+} as a common activating stimulus, they appear to have evolved distinct ways of tuning TM4-centered rearrangements to couple activation to diverse functional outputs.

Since TMEM16A is regulated not only by Ca^{2+} but also by PIP_2 (Le et al., 2019; Yu et al., 2019) and other factors, including alternative splicing (Ferrera et al., 2009), it will be interesting to investigate how these regulators affect the stability of the TM3–TM4 interaction. In addition, given that this hydrophobic patch contributes to the energetic stability of the conductive state, small molecules that alter the stability of this interaction network could provide a way to modulate TMEM16A gating without directly blocking the pore. More broadly, future studies may reveal whether TM3–TM4 interhelical interactions provide an additional layer of regulation that shapes TM4 rearrangement, thereby influencing the balance between ion conduction and lipid scrambling in TMEM16 scramblases. Consistent with this idea, remodeling of the TM3–TM4 interface by a mutation in the middle of TM3 in the fungal nhTMEM16 scramblase stabilizes an ion-conductive state (Khelashvili et al., 2019). Thus, TM3 and TM4 not only serve as structural gating helices, but may also form a regulatory interface through which TMEM16 proteins shape TM4 rearrangement and functional output.

Acknowledgments

Crina M. Nimigean served as an editor.

This work was supported by the Jiangsu Specially Appointed Professor Program and start-up funds from Nanjing Medical University (KY137R202531) to Z. Feng.

Author contributions: Zhang Feng: writing—original draft, review, and editing.

Disclosures: The author declares no competing interests exist.

References

Arndt, M., C. Alvadia, M.S. Straub, V. Clerico Mosina, C. Paulino, and R. Dutzler. 2022. Structural basis for the activation of the lipid scramblase TMEM16F. *Nat. Commun.* 13:6692. https://doi.org/10.1038/s41467-022-34497-x

Caputo, A., E. Caci, L. Ferrera, N. Pedemonte, C. Barsanti, E. Sondo, U. Pfeffer, R. Ravazzolo, O. Zegarra-Moran, and L.J.V. Galietta. 2008. TMEM16A, a membrane protein associated with calcium-dependent chloride channel activity. *Science* 322:590–594. https://doi.org/10.1126/science.1163518

Falzone, M.E., Z. Feng, O.E. Alvarenga, Y. Pan, B. Lee, X. Cheng, E. Fortea, S. Scheuring, and A. Accardi. 2022. TMEM16 scramblases thin the membrane to enable lipid scrambling. *Nat. Commun.* 13:2604. https://doi.org/10.1038/s41467-022-30300-z

Feng, S., S. Dang, T.W. Han, W. Ye, P. Jin, T. Cheng, J. Li, Y.N. Jan, L.Y. Jan, and Y. Cheng. 2019. Cryo-EM studies of TMEM16F calcium-activated ion channel suggest features important for lipid scrambling. *Cell Rep.* 28:1385. https://doi.org/10.1016/j.celrep.2019.07.052

Feng, Z., O.E. Alvarenga, E. Di Zanni, S. Lee, G. Khelashvili, and A. Accardi. 2026. Calcium dependent activation of the TMEM16F scramblase and ion channel. *Nat. Struct. Mol. Biol.* 33:664–676. https://doi.org/10.1038/s41594-026-01789-5

Feng, Z., E. Di Zanni, O. Alvarenga, S. Chakraborty, N. Rychlik, and A. Accardi. 2024. In or out of the groove? Mechanisms of lipid scrambling by TMEM16 proteins. *Cell Calcium.* 121:102896. https://doi.org/10.1016/j.ceca.2024.102896

Ferrera, L., A. Caputo, I. Ubby, E. Bussani, O. Zegarra-Moran, R. Ravazzolo, F. Pagani, and L.J. Galietta. 2009. Regulation of TMEM16A chloride channel properties by alternative splicing. *J. Biol. Chem.* 284:33360–33368. https://doi.org/10.1074/jbc.M109.046607

Kalienkova, V., V. Clerico Mosina, and C. Paulino. 2021. The groovy TMEM16 family: Molecular mechanisms of lipid scrambling and ion conduction. *J. Mol. Biol.* 433:166941. https://doi.org/10.1016/j.jmb.2021.166941

Khelashvili, G., M.E. Falzone, X. Cheng, B.C. Lee, A. Accardi, and H. Weinstein. 2019. Dynamic modulation of the lipid translocation groove generates a conductive ion channel in Ca^{2+}-bound nhTMEM16. *Nat. Commun.* 10:4972. https://doi.org/10.1038/s41467-019-12865-4

Kostritskii, A.Y., Y. Kostritskaia, N. Dmitrieva, T. Stauber, and J.P. Machtens. 2025. Calcium-activated chloride channel TMEM16A opens via pi-helical transition in transmembrane segment 4. *Proc. Natl. Acad. Sci. USA.* 122:e2421900122. https://doi.org/10.1073/pnas.2421900122

Kumar, P., and M. Bansal. 2015. Dissecting π-helices: Sequence, structure and function. *FEBS J.* 282:4415–4432. https://doi.org/10.1111/febs.13507

Lam, A.K.M., J. Rheinberger, C. Paulino, and R. Dutzler. 2021. Gating the pore of the calcium-activated chloride channel TMEM16A. *Nat. Commun.* 12:785. https://doi.org/10.1038/s41467-020-20787-9

Lam, A.K.M., S. Rutz, and R. Dutzler. 2022. Inhibition mechanism of the chloride channel TMEM16A by the pore blocker 1PBC. *Nat. Commun.* 13:2798. https://doi.org/10.1038/s41467-022-30479-1

Le, S.C., Z. Jia, J. Chen, and H. Yang. 2019. Molecular basis of PIP_2-dependent regulation of the Ca^{2+}-activated chloride channel TMEM16A. *Nat. Commun.* 10:3769. https://doi.org/10.1038/s41467-019-11784-8

Schroeder, B.C., T. Cheng, Y.N. Jan, and L.Y. Jan. 2008. Expression cloning of TMEM16A as a calcium-activated chloride channel subunit. *Cell.* 134:1019–1029. https://doi.org/10.1016/j.cell.2008.09.003

Stephens, C.A., F.V. Marcoline, C.J. Peters, and M. Grabe. 2026. Conformational changes upon pore blocker removal reveal conductive states of TMEM16A. *J. Gen. Physiol.* 158:e202513961. https://doi.org/10.1085/jgp.202513961

Yang, Y.D., H. Cho, J.Y. Koo, M.H. Tak, Y. Cho, W.S. Shim, S.P. Park, J. Lee, B. Lee, B.M. Kim, et al. 2008. TMEM16A confers receptor-activated calcium-dependent chloride conductance. *Nature.* 455:1210–1215. https://doi.org/10.1038/nature07313

Yu, K., T. Jiang, Y. Cui, E. Tajkhorshid, and H.C. Hartzell. 2019. A network of phosphatidylinositol 4,5-bisphosphate binding sites regulates gating of the Ca^{2+}-activated Cl^- channel ANO1 (TMEM16A). *Proc. Natl. Acad. Sci. USA.* 116:19952–19962. https://doi.org/10.1073/pnas.1904012116